Atmospheric Definition for Shuttle Aerothermodynamic Investigations

Joseph M. Price*
NASA Langley Research Center, Hampton, Virginia

A procedure has been developed to estimate the freestream atmospheric properties along the Shuttle trajectory during atmospheric re-entry. The procedure utilizes measurement data obtained by NASA, NOAA, and the Air Force, and model data for regions where measured data are nonexistent. The results obtained are used to determine the best atmosphere-relative trajectory parameters during re-entry and to allow for an evaluation of the aerodynamic and aerothermodynamic characteristics of the Shuttle. A discussion of the method employed by the Langley Atmospheric Information Retrieval System, which is a computer code for the determination of atmospheric parameters, is presented. Results obtained from the first two Shuttle flights, STS-1 and STS-2, are also given with applications of these atmospheric parameters.

Nomenclature

C_N	= normal force coefficient
$f(Z)$	= density or pressure at altitude Z
$\bar{M}(Z)$	= mean molecular weight at altitude Z
N_A	= Avogadro's number
$n_\ell(Z)$	= number density of individual species l at altitude Z
$P(Z)$	= pressure at altitude Z
R^*	= universal gas constant
$T(Z)$	= temperature at altitude Z
Z	= altitude
$\rho(Z)$	= density at altitude Z

Introduction

EVALUATION of the aerodynamic performance of the Shuttle during atmospheric re-entry requires a determination of the freestream atmospheric properties along the entry path. This determination must be of the best possible accuracy in order to fully utilize the Shuttle as an aerodynamic flight research vehicle. To accomplish this, two Shuttle Orbiter experiments, the Shuttle Upper Atmosphere Mass Spectrometer (SUMS),[1,2] and the Shuttle Entry Air Data System (SEADS),[2] are being developed to provide onboard measurements. SUMS will measure freestream parameters in the high altitude (>66 km), high Mach number ($M>17$) regions where conventional static pressure measurements are not available. SEADS will provide research quality data below about 90 km. Until SEADS and SUMS are fully developed and integrated into the Shuttle for flight, an alternate method is needed to determine the freestream atmospheric properties along the entry trajectory. Such a method was developed and is described in this paper.

Meteorological Data

NASA has provided for the National Oceanic and Atmospheric Administration (NOAA) to obtain soundings of meteorological data close to the times of Shuttle ascent and descent from a network of suitably located stations. Of particular interest for the present discussions are those soundings taken in the vicinity of Shuttle re-entry at Barking Sands, Hawaii, Point Mugu, California, and especially the data taken at Edwards Air Force Base, California by the Air Force and NASA near the time of landing. These locations are shown relative to the Shuttle STS-1 and STS-2 ground track in Fig. 1.

Three different measurement systems were used for obtaining meteorological data. They were the Rawinsonde from the surface to 30 km, rocketsonde from 30 to 70 km, and meteorological spheres from 60 to 90 km. The Rawinsonde is a balloon that rises with onboard temperature and pressure sensors. The pressure sensor is calibrated to the station pressure measurement before the balloon is released. The altitude is then determined from the pressure level measurement using standard atmosphere tables and the density is calculated from the temperature and pressure.

The rocketsonde consists of a temperature sensor that is released from a rocket at about 70 km to fall with a parachute and be tracked by radar. The pressure level is determined at the bottom of the region by comparing with Rawinsonde data taken near the same time and place. This is then used to calculate the atmospheric parameters up through the covered altitude range. Wind information is obtained from radar tracking of the parachute drift.

The meteorological sphere is a 1-m inflatable sphere that is released from a rocket at approximately 110 km and tracked by radar. Useful drag information is obtained beginning at about 90 km down to about 60 km. From this drag, the density is determined as a function of altitude. Radar tracking of the sphere provides wind parameters. The present analysis is based on atmospheric parameters calculated from meteorological sphere data taken at Barking Sands, rocketsonde data taken at Point Mugu, and Rawinsonde data taken at Edwards. The data at each location are provided over an altitude range as illustrated in Fig. 2a for flight 1 and Fig. 2b for flight 2.

Langley Atmospheric Information Retrieval System

The model approximating the freestream atmospheric properties along the Shuttle trajectory during atmospheric entry is obtained using a computer code called the Langley Atmospheric Information Retrieval System (LAIRS).[3,4] The principal task of the LAIRS software is to transfer the measurement data from the remote stations to the Shuttle track. This is done using diurnal, semidiurnal, and latitudinal

Received April 13, 1982; revision received Sept. 7, 1982. This paper is declared a work of the U.S. Government and therefore is in the public domain.

*Mathematician, Aerothermodynamics Branch, Space Systems Division. Member AIAA.

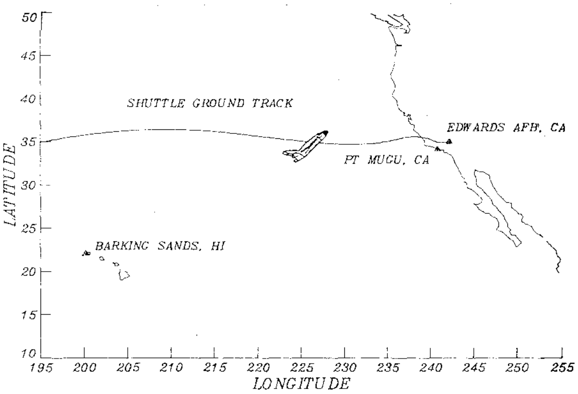

Fig. 1 Meteorological data stations for Shuttle.

variations obtained from reference atmospheric models. Any other longitudinal variations are neglected. The uncertainties associated with the translation of the atmospheric parameters are reduced as the time and distance between the Shuttle and the measurement time and location are reduced. The atmospheres being presented in this paper are the result of a two-step execution of the LAIRS software.

Step 1

The first step in LAIRS is to produce the most straightforward model, which consists of determining by interpolation the atmospheric parameters at points along the Shuttle trajectory.[5] First, the temperature data are interpolated in altitude with second-order Lagrangian interpolation. It is assumed that the pressure and density vary logarithmically with altitude. These values are interpolated using the following relationship:

$$f(Z)=f(Z_i)\exp\left[\frac{Z_i-Z}{Z_i-Z_{i+1}}\ln\left(\frac{f(Z_{i+1})}{f(Z_i)}\right)\right] \qquad Z_i\leq Z\leq Z_{i+1} \qquad (1)$$

where f represents the altitude-dependent parameter.

After each profile has been interpolated in altitude, the points from each profile corresponding to a given altitude are interpolated again in latitude and local solar time. For this, the longitude and Greenwich Mean Time (GMT) for each profile are converted to local solar times. A bivariate second-order Lagrangian interpolation is then performed. The model incorporates the latitude gradients and diurnal and semidiurnal coefficients for temperature, pressure, and density obtained from the COSPAR International Reference Atmosphere 1972[6] above 25 km. Below this altitude, diurnal and semidiurnal variations are assumed to be zero and the latitude gradients are obtained from the Handbook of Geophysics and Space Environments.[7] Wind data are linearly interpolated in altitude from the closest available measured profile. No attempt is made to correct the winds for latitude and longitude differences. Consequently, the uncertainties in the wind information are greatly increased as the distance from the Shuttle to the measurement location increases.

Since measured data are not available significantly above 90 km, the Jacchia-Roberts model[8,9] is used in this region as a model for the atmosphere with the boundary values chosen to match the meteorological profiles below 90 km. The Jacchia-Roberts model determines the atmospheric mass density, ρ, from the barometric equation in the region below 100 km where the atmosphere is homogeneously mixed. Above this region, where the lighter species separate from heavier species by the process of molecular diffusion, the number densities of individual species are determined from the diffusion equation. The temperature height profile used in the Jacchia-Roberts model was empirically obtained in the Jacchia 1971 model and slightly modified by Roberts in the present model so that the density equations can be analytically integrated. This temperature profile takes the form of a fourth-order polynomial for heights from 90 to 125 km and an exponential function of altitude for heights above 125 km. The pressure values for the Jacchia-Roberts model are then obtained from the following relations:

$$P(Z)=R^*T(Z)\sum_{\ell}\frac{n_\ell(Z)}{N_A} \qquad Z>100\text{ km}$$

$$=R^*T(Z)\frac{\rho(Z)}{\bar{M}(Z)} \qquad Z\leq 100\text{ km} \qquad (2)$$

Step 2

The second step in the derivation of the model being presented requires an additional execution of the LAIRS software. This time the model obtained from the previous execution is input as if it were an observation profile. The Jacchia-Roberts model is again employed for altitudes above 90 km; however, a fitted polynomial model is used in the region below 90 km. In this scheme, the lower atmosphere is divided into three segments (0-25 km, 24-65 km, and 65-90 km). The logarithms of the pressure and density from the previous execution of LAIRS are fit to polynomials separately in each segment of the atmosphere. This is done using a linear least-square fitting procedure. The temperature is then calculated from the pressure and density values so that the gas law is satisfied. The interpolated wind data are unchanged.

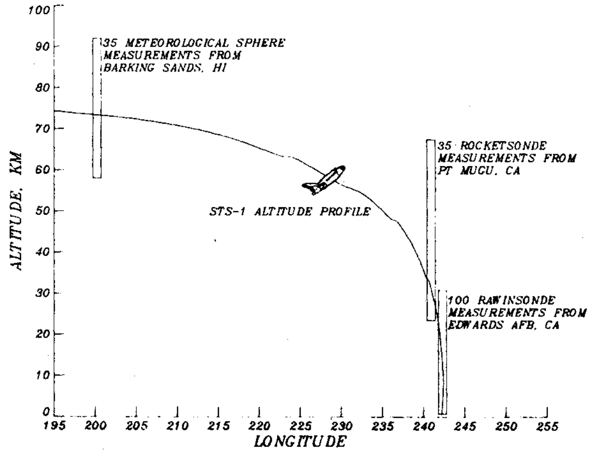

a)

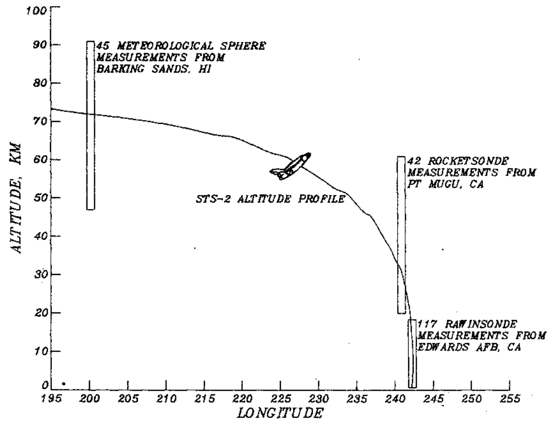

b)

Fig. 2 Altitude range of meteorological data sources. a) STS-1; b) STS-2.

Atmosphere Encountered During Shuttle Re-entry

The temperature, pressure, density, and wind profiles encountered by STS-1 as computed by LAIRS are given in Table 1 and those profiles from STS-2 are presented in Table 2. The temperature profiles generated along the track of the Shuttle by LAIRS are shown in Fig. 3. The residuals between these profiles and the interpolated profiles from step 1 for each flight are nowhere more than about 10 deg with much smaller residuals in the vicinity of Edwards. NOAA has provided NASA with five vertical profiles at specified locations along the track of the Shuttle. These profiles were obtained by NOAA using the same measurements with additional information provided by local daily weather maps and NOAA personnel with expertise in translating the data to the specified locations. At these particular locations where NOAA vertical profiles cross the LAIRS along-track profile, the temperature agreement is within 0.3-7.0 deg, with the best agreement near Edwards as expected. This is well within the uncertainties of either the LAIRS or the NOAA temperatures. The fact that both methods yield essentially the same values at

Table 1 LAIRS atmospheric parameters for STS-1

Altitude, km	Latitude, deg	Longitude, deg	Temperature, K	Pressure, N/m^2	Density, kg/m^3	E-W wind, m/s	N-S wind, m/s
89.79	27.6	173.5	190	0.178E+00	0.328E−05	28.5	−0.3
87.92	28.1	174.4	188	0.248E+00	0.459E−05	−3.9	16.5
86.11	28.6	175.3	188	0.341E+00	0.632E−05	−23.0	27.1
84.38	29.1	176.2	189	0.463E+00	0.854E−05	−29.0	31.4
82.77	29.6	177.1	191	0.614E+00	0.112E−04	−29.0	28.3
81.31	30.0	178.0	193	0.791E+00	0.143E−04	−27.6	19.8
80.04	30.5	179.0	195	0.985E+00	0.176E−04	−26.5	8.5
78.98	30.9	179.9	196	0.118E+01	0.209E−04	−24.9	−1.9
78.18	31.4	180.9	198	0.135E+01	0.238E−04	−23.1	−9.9
77.59	31.8	181.8	199	0.149E+01	0.262E−04	−21.3	−15.3
77.15	32.3	182.8	199	0.161E+01	0.281E−04	−19.6	−19.1
76.82	32.7	183.8	200	0.170E+01	0.296E−04	−18.3	−21.9
76.51	33.1	184.7	201	0.179E+01	0.311E−04	−16.9	−24.5
76.22	33.4	185.7	201	0.188E+01	0.325E−04	−15.6	−26.9
75.94	33.8	186.7	201	0.196E+01	0.340E−04	−14.2	−28.8
75.70	34.2	187.7	202	0.205E+01	0.353E−04	−12.8	−30.4
75.49	34.5	188.7	202	0.212E+01	0.365E−04	−11.5	−31.6
75.30	34.9	189.7	203	0.219E+01	0.376E−04	−10.4	−32.6
75.11	35.2	190.8	203	0.226E+01	0.387E−04	−9.2	−33.5
74.91	35.5	191.8	203	0.233E+01	0.399E−04	−7.9	−34.3
74.72	35.8	192.8	203	0.240E+01	0.412E−04	−6.6	−35.0
74.52	36.0	193.8	204	0.248E+01	0.425E−04	−5.1	−35.8
74.31	36.3	194.9	204	0.257E+01	0.439E−04	−3.6	−36.3
74.10	36.5	195.9	204	0.266E+01	0.453E−04	−2.0	−36.6
73.89	36.8	197.0	205	0.275E+01	0.469E−04	−0.5	−36.8
73.69	37.0	198.0	205	0.284E+01	0.483E−04	1.0	−36.9
73.51	37.2	199.0	205	0.293E+01	0.497E−04	2.5	−36.8
73.32	37.3	200.1	205	0.302E+01	0.512E−04	4.0	−36.5
73.12	37.5	201.1	206	0.312E+01	0.528E−04	5.4	−36.1
72.93	37.7	202.2	206	0.322E+01	0.545E−04	6.8	−35.6
72.72	37.8	203.2	206	0.333E+01	0.563E−04	8.4	−34.9
72.47	37.9	204.3	207	0.347E+01	0.585E−04	10.1	−33.9
72.20	38.0	205.3	207	0.362E+01	0.610E−04	12.0	−32.6
71.90	38.1	206.4	207	0.380E+01	0.640E−04	14.0	−30.7
71.58	38.2	207.4	207	0.400E+01	0.672E−04	16.2	−28.4
71.26	38.2	208.4	208	0.421E+01	0.706E−04	18.4	−25.3
70.91	38.3	209.5	208	0.445E+01	0.746E−04	20.5	−22.3
70.53	38.3	210.5	208	0.474E+01	0.792E−04	22.6	−18.6
70.13	38.3	211.5	209	0.505E+01	0.843E−04	24.4	−14.6
69.72	38.3	212.5	209	0.539E+01	0.900E−04	26.3	−10.6
69.27	38.3	213.5	209	0.580E+01	0.966E−04	28.1	−5.8
68.78	38.2	214.5	209	0.627E+01	0.104E−03	30.1	−2.0
68.28	38.2	215.4	209	0.679E+01	0.113E−03	31.9	0.8
67.75	38.1	216.4	211	0.739E+01	0.122E−03	33.9	3.4
67.17	38.0	217.3	215	0.810E+01	0.131E−03	26.6	−0.5
66.53	37.9	218.3	219	0.894E+01	0.142E−03	27.6	−0.4
65.86	37.8	219.2	223	0.989E+01	0.155E−03	31.1	1.8
65.18	37.7	220.1	227	0.110E+02	0.168E−03	33.4	4.6
64.49	37.6	221.0	230	0.121E+02	0.183E−03	34.6	6.9
63.84	37.4	221.8	234	0.133E+02	0.198E−03	34.6	9.8
63.28	37.3	222.7	236	0.144E+02	0.213E−03	33.9	11.3
63.13	37.1	223.5	237	0.147E+02	0.216E−03	33.6	11.3
62.78	36.9	224.3	238	0.155E+02	0.226E−03	32.8	11.4
62.03	36.8	225.1	242	0.172E+02	0.248E−03	30.1	10.7
61.11	36.6	225.9	245	0.195E+02	0.277E−03	23.7	8.8
60.23	36.5	226.7	248	0.220E+02	0.308E−03	21.9	7.2
59.36	36.4	227.4	251	0.247E+02	0.343E−03	25.8	3.7
58.47	36.3	228.1	253	0.278E+02	0.382E−03	29.4	2.1
57.64	36.2	228.8	255	0.310E+02	0.423E−03	34.9	1.5
56.85	36.1	229.5	257	0.344E+02	0.466E−03	38.5	3.6
56.15	36.0	230.2	258	0.377E+02	0.508E−03	40.4	6.1

(Table 1 continued on next page)

Table 1 Continued

Altitude, km	Latitude, deg	Longitude, deg	Temperature, K	Pressure, N/m^2	Density, kg/m^3	E-W wind, m/s	N-S wind, m/s
55.67	35.9	230.8	259	0.401*E*+02	0.539*E*−03	41.0	8.1
55.22	35.9	231.5	260	0.425*E*+02	0.570*E*−03	41.1	9.8
54.68	35.8	232.1	260	0.456*E*+02	0.609*E*−03	40.4	11.1
54.01	35.8	232.7	261	0.497*E*+02	0.662*E*−03	38.6	12.0
53.24	35.8	233.2	262	0.548*E*+02	0.729*E*−03	35.1	12.2
52.35	35.8	233.8	263	0.614*E*+02	0.815*E*−03	28.5	11.3
51.42	35.8	234.3	263	0.692*E*+02	0.916*E*−03	28.4	5.3
50.44	35.8	234.8	263	0.785*E*+02	0.104*E*−02	28.2	−0.4
49.38	35.9	235.3	263	0.899*E*+02	0.119*E*−02	27.7	−2.7
48.50	35.9	235.7	263	0.101*E*+03	0.133*E*−02	28.8	−1.6
47.85	36.0	236.2	262	0.109*E*+03	0.145*E*−02	28.3	0.1
47.61	36.0	236.6	262	0.113*E*+03	0.150*E*−02	28.0	0.9
46.88	36.1	237.0	262	0.124*E*+03	0.165*E*−02	26.0	4.9
45.76	36.1	237.4	261	0.143*E*+03	0.191*E*−02	22.3	10.6
44.61	36.1	237.8	259	0.166*E*+03	0.223*E*−02	21.2	5.3
43.51	36.1	238.1	258	0.192*E*+03	0.259*E*−02	18.9	0.8
42.38	36.0	238.4	256	0.222*E*+03	0.302*E*−02	17.6	−2.4
41.19	36.0	238.8	254	0.260*E*+03	0.356*E*−02	17.0	−8.0
40.02	35.9	239.0	252	0.304*E*+03	0.420*E*−02	18.5	−11.5
38.86	35.9	239.3	250	0.355*E*+03	0.495*E*−02	20.6	−10.2
37.68	35.8	239.6	248	0.417*E*+03	0.586*E*−02	22.1	−6.9
36.50	35.7	239.8	245	0.490*E*+03	0.696*E*−02	23.0	−6.9
35.39	35.6	240.0	243	0.571*E*+03	0.818*E*−02	21.1	−9.1
34.35	35.5	240.2	241	0.661*E*+03	0.956*E*−02	14.8	−12.8
33.59	35.4	240.4	239	0.735*E*+03	0.107*E*−01	10.7	−15.4
33.19	35.3	240.5	238	0.778*E*+03	0.114*E*−01	9.2	−16.7
32.44	35.2	240.7	237	0.866*E*+03	0.128*E*−01	7.1	−18.7
31.28	35.1	240.9	234	0.102*E*+04	0.152*E*−01	4.0	−16.9
30.05	35.1	241.0	232	0.122*E*+04	0.184*E*−01	1.7	−8.0
28.84	35.1	241.2	229	0.146*E*+04	0.222*E*−01	−2.5	−8.3
27.63	35.0	241.3	227	0.175*E*+04	0.268*E*−01	−4.8	−7.9
26.40	35.0	241.4	225	0.210*E*+04	0.326*E*−01	−3.8	−8.2
25.25	35.1	241.5	223	0.250*E*+04	0.392*E*−01	−10.2	−5.6
24.41	35.1	241.6	221	0.285*E*+04	0.448*E*−01	−8.5	−2.8
23.51	35.1	241.7	220	0.327*E*+04	0.518*E*−01	−8.3	−2.3
22.36	35.0	241.8	218	0.390*E*+04	0.622*E*−01	−3.3	−2.2
21.07	35.0	241.9	217	0.477*E*+04	0.766*E*−01	2.8	1.8
19.79	35.0	242.0	216	0.584*E*+04	0.942*E*−01	4.4	6.5
18.59	35.0	242.0	215	0.705*E*+04	0.114*E*+00	7.4	4.9
17.44	35.0	242.1	215	0.846*E*+04	0.137*E*+00	9.5	11.2
16.39	35.0	242.1	215	0.999*E*+04	0.162*E*+00	8.6	10.8
15.35	35.0	242.2	215	0.118*E*+05	0.191*E*+00	11.9	10.3
14.34	34.9	242.2	216	0.138*E*+05	0.223*E*+00	13.3	9.3
13.42	34.9	242.2	215	0.160*E*+05	0.259*E*+00	10.6	6.2
12.50	34.9	242.3	214	0.185*E*+05	0.300*E*+00	12.7	3.8
11.57	34.9	242.3	216	0.214*E*+05	0.345*E*+00	11.2	0.2
10.59	34.9	242.4	219	0.249*E*+05	0.396*E*+00	9.6	−5.0
9.56	34.9	242.4	225	0.292*E*+05	0.452*E*+00	7.4	−2.0
8.60	34.9	242.4	232	0.337*E*+05	0.506*E*+00	4.6	0.1
7.74	35.0	242.4	239	0.382*E*+05	0.558*E*+00	2.1	0.6
6.92	35.0	242.4	245	0.429*E*+05	0.608*E*+00	0.9	−1.1
6.20	35.0	242.4	252	0.473*E*+05	0.655*E*+00	−0.3	−0.4
5.54	35.0	242.3	258	0.517*E*+05	0.699*E*+00	1.4	2.0
4.65	35.0	242.3	265	0.580*E*+05	0.762*E*+00	1.1	4.1
3.72	35.0	242.3	273	0.653*E*+05	0.833*E*+00	−2.6	5.2
2.87	35.0	242.3	279	0.725*E*+05	0.904*E*+00	−5.4	3.7
2.03	35.0	242.2	285	0.802*E*+05	0.981*E*+00	−5.6	2.1
1.28	35.0	242.2	289	0.878*E*+05	0.106*E*+01	−3.3	0.8
0.70	35.0	242.2	292	0.940*E*+05	0.112*E*+01	0.0	0.0
0.65	35.0	242.2	292	0.945*E*+05	0.113*E*+01	0.0	0.0
0.64	35.0	242.2	292	0.946*E*+05	0.113*E*+01	0.0	0.0

the particular locations where they can be directly compared tends to corroborate both methods of reducing the basic data.[10]

The density and pressure profiles generated using LAIRS are shown in Figs. 4 and 5. They agree with the NOAA vertical profiles at the crossing points to within 0.8 to 7.8% above 30 km and less than 1% at lower altitudes. Studies performed at the Langley Research Center to extract the normal-force coefficients, C_N, for the Shuttle have uncovered some differences in the flight and predicted C_N values.[11] These differences occur in the altitude range from 56 to 75 km, especially on flight 2. One possible source for the discrepancies is the density measurements from the meteorological spheres in this altitude range. The NOAA results reflect these same differences since they are obtained from the same measurement sources. Another possible explanation would be an unexpected flowfield phenomenon in the Mach 14-25 range, which would indicate an error in the predicted values. This difference is a major concern of the Shuttle aerodynamics community and every effort is being

Table 2 LAIRS atmospheric parameters for STS-2

Altitude, km	Latitude, deg	Longitude, deg	Temperature, K	Pressure, N/m^2	Density, kg/m^3	E-W wind, m/s	N-S wind, m/s
88.42	27.0	173.1	189	0.230E+00	0.423E−05	−12.8	−60.1
86.61	27.5	174.0	197	0.314E+00	0.555E−05	−11.6	−56.2
84.87	27.9	174.9	200	0.419E+00	0.729E−05	−1.2	−31.8
83.23	28.4	175.8	202	0.550E+00	0.950E−05	10.7	−7.1
81.70	28.8	176.7	202	0.708E+00	0.122E−04	17.6	8.4
80.31	29.2	177.7	201	0.892E+00	0.155E−04	20.9	11.9
79.10	29.7	178.6	200	0.109E+01	0.190E−04	22.0	8.0
78.08	30.1	179.6	199	0.129E+01	0.226E−04	21.3	1.1
77.30	30.5	180.6	199	0.147E+01	0.258E−04	19.9	−5.7
76.76	30.9	181.5	198	0.161E+01	0.284E−04	18.6	−10.6
76.34	31.3	182.5	198	0.173E+01	0.304E−04	17.3	−14.7
76.03	31.6	183.5	198	0.182E+01	0.321E−04	16.4	−17.3
75.84	32.0	184.5	198	0.188E+01	0.331E−04	15.9	−18.8
75.70	32.3	185.5	198	0.193E+01	0.339E−04	15.6	−19.7
75.54	32.7	186.5	198	0.198E+01	0.348E−04	15.2	−20.8
75.35	33.0	187.5	198	0.205E+01	0.360E−04	14.7	−22.2
75.12	33.3	188.5	198	0.213E+01	0.374E−04	14.2	−23.4
74.87	33.6	189.5	198	0.222E+01	0.389E−04	13.8	−24.3
74.61	33.9	190.5	199	0.232E+01	0.407E−04	13.3	−24.9
74.31	34.1	191.5	199	0.244E+01	0.427E−04	12.9	−25.3
74.01	34.4	192.6	199	0.256E+01	0.449E−04	12.7	−24.9
73.70	34.6	193.6	199	0.270E+01	0.472E−04	12.5	−23.8
73.40	34.8	194.6	200	0.284E+01	0.495E−04	12.3	−22.0
73.09	35.0	195.7	200	0.299E+01	0.520E−04	12.5	−19.6
72.76	35.2	196.7	201	0.316E+01	0.547E−04	13.0	−16.1
72.46	35.4	197.7	202	0.332E+01	0.573E−04	13.7	−12.3
72.20	35.6	198.8	202	0.347E+01	0.597E−04	14.7	−8.1
71.96	35.7	199.8	203	0.360E+01	0.618E−04	15.4	−4.4
71.75	35.9	200.8	204	0.373E+01	0.638E−04	15.9	−0.9
71.54	36.0	201.9	204	0.386E+01	0.658E−04	16.5	2.8
71.31	36.1	202.9	205	0.401E+01	0.681E−04	16.9	7.8
71.06	36.2	203.9	206	0.417E+01	0.706E−04	17.8	12.2
70.80	36.2	205.0	207	0.435E+01	0.732E−04	18.8	16.6
70.53	36.3	206.0	208	0.455E+01	0.761E−04	20.1	21.1
70.23	36.3	207.0	210	0.477E+01	0.793E−04	21.9	26.6
69.93	36.4	208.0	211	0.500E+01	0.825E−04	23.5	30.1
69.65	36.4	209.0	213	0.523E+01	0.857E−04	25.0	32.7
69.30	36.4	210.0	215	0.552E+01	0.896E−04	27.0	35.1
68.93	36.4	211.0	217	0.585E+01	0.938E−04	28.9	35.6
68.54	36.3	212.0	220	0.621E+01	0.984E−04	30.7	34.1
68.13	36.3	212.9	223	0.661E+01	0.103E−03	32.2	29.6
67.71	36.2	213.9	226	0.704E+01	0.109E−03	34.3	25.1
67.23	36.2	214.8	228	0.755E+01	0.115E−03	37.0	18.1
66.77	36.1	215.8	230	0.807E+01	0.122E−03	39.2	12.9
66.41	36.0	216.7	232	0.850E+01	0.128E−03	40.9	8.8
66.30	35.9	217.6	233	0.864E+01	0.129E−03	41.4	7.8
66.06	35.7	218.5	234	0.895E+01	0.133E−03	42.4	6.0
65.58	35.6	219.4	236	0.957E+01	0.141E−03	44.3	3.7
64.92	35.5	220.3	239	0.105E+02	0.153E−03	46.8	3.2
64.18	35.4	221.1	242	0.117E+02	0.168E−03	50.7	3.8
63.43	35.3	222.0	244	0.129E+02	0.184E−03	54.4	1.8
62.67	35.3	222.8	247	0.143E+02	0.202E−03	56.7	0.9
61.98	35.2	223.6	249	0.157E+02	0.220E−03	57.1	1.8
61.45	35.1	224.4	251	0.169E+02	0.235E−03	56.4	5.7
61.10	35.0	225.2	251	0.177E+02	0.245E−03	55.3	10.1
60.61	34.9	226.0	253	0.189E+02	0.261E−03	54.2	−6.6
59.76	34.9	226.7	255	0.211E+02	0.289E−03	54.0	−3.5
58.75	34.8	227.5	257	0.241E+02	0.327E−03	52.7	3.7
57.84	34.8	228.2	258	0.272E+02	0.366E−03	55.0	−5.9
57.00	34.7	228.9	259	0.303E+02	0.407E−03	59.7	−4.7
56.12	34.7	229.6	260	0.340E+02	0.454E−03	62.0	−2.5
55.27	34.7	230.2	261	0.379E+02	0.505E−03	60.9	−3.7

(Table 2 continued on next page)

Table 2 Continued

Altitude, km	Latitude, deg	Longitude, deg	Temperature, K	Pressure, N/m^2	Density, kg/m^3	E-W wind, m/s	N-S wind, m/s
54.40	34.7	230.9	262	0.423E+02	0.563E−03	59.4	−2.6
53.51	34.7	231.5	262	0.475E+02	0.631E−03	57.7	1.1
52.70	34.7	232.1	262	0.527E+02	0.699E−03	55.7	5.1
52.16	34.7	232.7	262	0.564E+02	0.749E−03	52.9	5.1
51.80	34.8	233.2	262	0.591E+02	0.785E−03	50.7	4.8
51.21	34.8	233.7	262	0.637E−02	0.847E−03	46.4	3.5
50.26	34.9	234.2	262	0.720E+02	0.958E−03	41.1	0.8
49.17	35.0	234.7	261	0.828E+02	0.110E−02	36.2	−5.1
48.09	35.0	235.2	260	0.952E+02	0.127E−02	33.0	−9.1
47.20	35.1	235.6	260	0.107E+03	0.143E−02	32.2	−10.3
46.34	35.2	236.1	259	0.120E+03	0.161E−02	31.0	−9.2
45.86	35.3	236.4	258	0.127E+03	0.172E−02	29.4	−7.7
45.38	35.4	236.8	257	0.135E+03	0.183E−02	24.7	−5.8
44.42	35.5	237.2	256	0.154E+03	0.209E−02	15.9	−6.8
43.32	35.5	237.6	254	0.178E+03	0.244E−02	11.0	−8.1
42.06	35.6	237.9	252	0.210E+03	0.290E−02	13.5	−5.5
40.94	35.6	238.2	250	0.244E+03	0.340E−02	8.3	−6.9
39.91	35.6	238.6	248	0.281E+03	0.394E−02	3.1	−10.4
38.92	35.5	238.9	246	0.321E+03	0.455E−02	3.9	−12.8
37.98	35.5	239.1	244	0.366E+03	0.522E−02	5.2	−11.3
37.07	35.5	239.4	242	0.415E+03	0.598E−02	3.4	−7.9
36.06	35.4	239.7	240	0.478E+03	0.695E−02	2.8	−6.6
35.02	35.3	239.9	238	0.554E+03	0.813E−02	−0.6	−9.6
34.07	35.2	240.1	235	0.635E+03	0.940E−02	−4.3	−9.9
33.34	35.2	240.3	234	0.705E+03	0.105E−01	−5.2	−8.2
32.83	35.1	240.5	233	0.760E+03	0.114E−01	−5.2	−6.6
32.20	35.0	240.6	231	0.833E+03	0.125E−01	−4.3	−4.4
31.49	35.0	240.8	230	0.923E+03	0.140E−01	−4.4	−3.0
30.51	34.9	241.0	228	0.107E+04	0.164E−01	−6.3	−2.6
29.34	34.9	241.1	225	0.127E+04	0.197E−01	−7.6	−3.2
28.16	34.9	241.2	223	0.152E+04	0.238E−01	−3.0	−3.4
27.02	34.9	241.4	220	0.181E+04	0.286E−01	−0.4	−4.1
25.81	34.9	241.5	218	0.218E+04	0.349E−01	2.0	−2.4
24.76	35.0	241.6	216	0.257E+04	0.414E−01	3.4	−1.2
23.80	35.0	241.7	215	0.299E+04	0.486E−01	2.9	−0.8
22.84	35.0	241.8	213	0.349E+04	0.570E−01	2.5	−0.6
21.91	35.0	241.9	212	0.404E+04	0.665E−01	2.9	−1.1
20.93	35.0	241.9	211	0.473E+04	0.781E−01	3.8	−2.7
19.81	35.0	242.0	210	0.567E+04	0.943E−01	10.6	−2.9
18.47	35.0	242.1	208	0.705E+04	0.118E+00	20.8	−3.2
17.09	34.9	242.1	208	0.882E+04	0.148E+00	22.5	0.5
15.81	34.9	242.2	207	0.109E+05	0.183E+00	35.0	0.1
14.52	34.9	242.2	207	0.135E+05	0.226E+00	27.6	−0.5
13.34	34.9	242.3	210	0.163E+05	0.271E+00	42.5	−6.5
12.10	34.9	242.3	215	0.199E+05	0.322E+00	42.9	−10.7
10.63	34.9	242.3	224	0.250E+05	0.390E+00	42.3	−2.3
9.08	34.9	242.4	234	0.315E+05	0.469E+00	34.1	4.8
7.67	34.9	242.4	245	0.385E+05	0.547E+00	37.9	5.9
6.51	35.0	242.4	254	0.451E+05	0.618E+00	29.4	0.5
5.75	35.0	242.4	260	0.499E+05	0.668E+00	25.8	1.3
5.07	35.0	242.4	265	0.544E+05	0.715E+00	20.4	3.8
4.48	35.0	242.4	270	0.587E+05	0.758E+00	17.5	3.6
3.88	35.0	242.3	274	0.633E+05	0.804E+00	17.9	1.9
3.58	35.0	242.3	276	0.657E+05	0.828E+00	17.9	2.2
3.27	35.0	242.3	279	0.683E+05	0.854E+00	17.8	2.9
3.01	35.0	242.3	280	0.705E+05	0.876E+00	17.8	2.6
2.61	35.0	242.3	283	0.740E+05	0.911E+00	17.2	1.0
2.19	35.0	242.2	285	0.778E+05	0.950E+00	15.2	−0.3
1.74	35.0	242.2	288	0.821E+05	0.993E+00	11.1	0.7
1.12	35.0	242.2	291	0.883E+05	0.106E+01	10.0	4.0
0.72	35.0	242.2	293	0.925E+05	0.110E+01	7.3	7.8
0.64	35.0	242.2	293	0.934E+05	0.111E+01	6.5	8.1

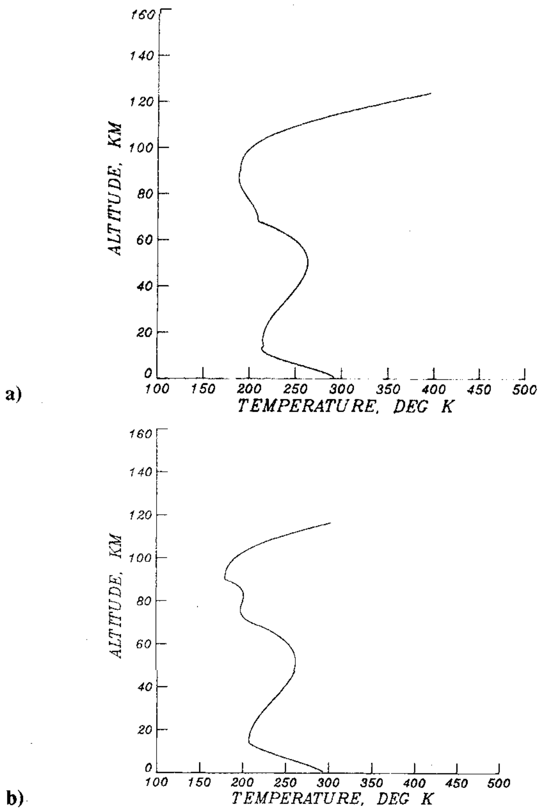

Fig. 3 Temperature profile. a) STS-1; b) STS-2.

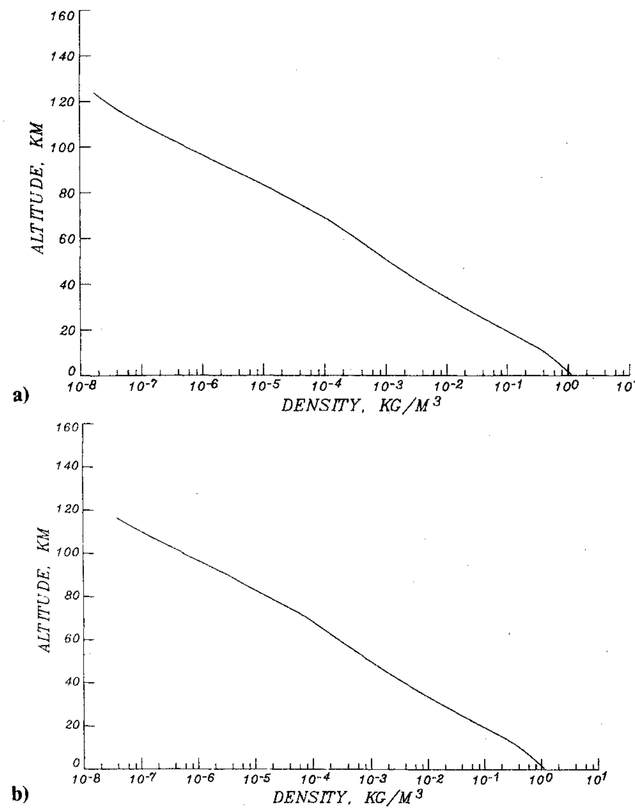

Fig. 4 Density profile. a) STS-1; b) STS-2.

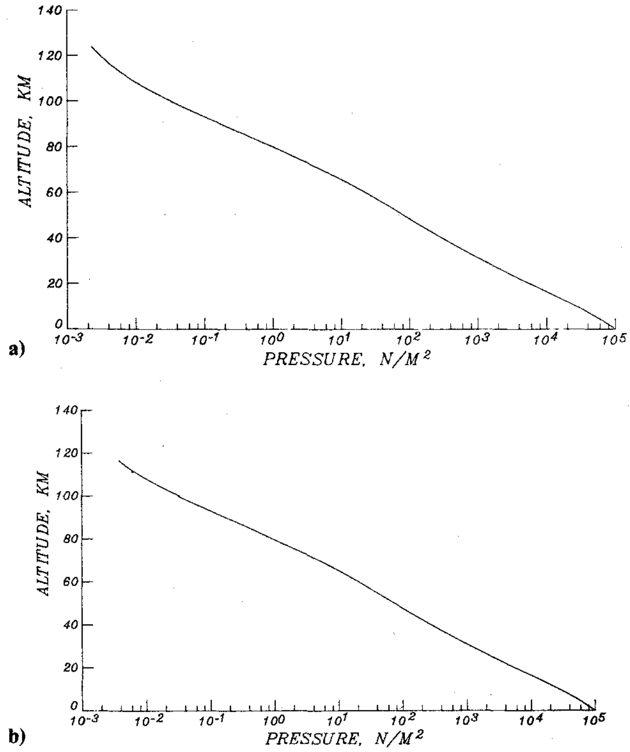

Fig. 5 Pressure profile. a) STS-1; b) STS-2.

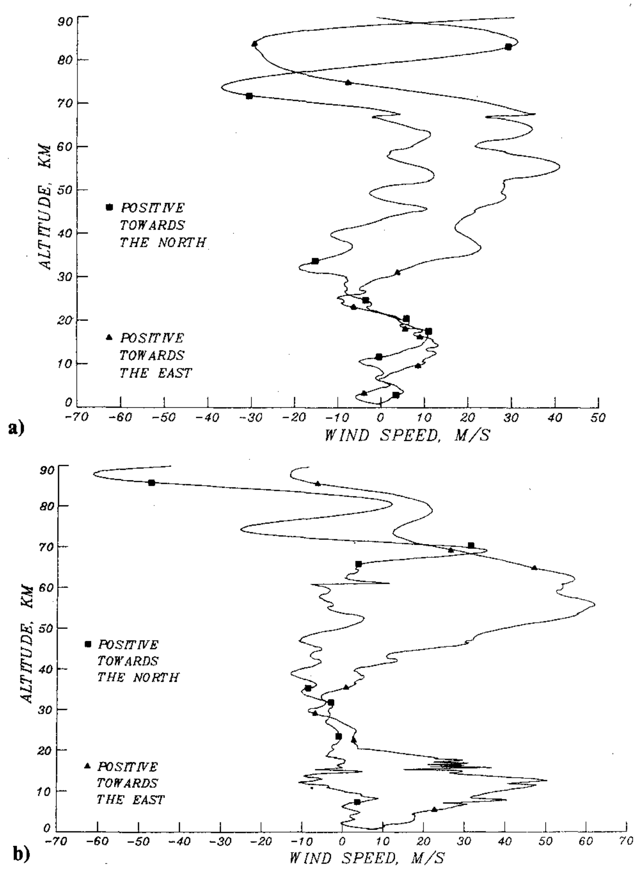

Fig. 6 N-S, E-W wind speed. a) STS-1; b) STS-2.

made to understand the source.

In addition to knowing the temperature, density, and pressure, it is extremely important to the STS trajectory reconstruction process to properly account for winds. This is especially true over the altitude range for which the planet-relative spacecraft velocity is not dominant compared to the wind velocity. This altitude range is generally the lowest at 15 km. The horizontal winds measured near the time of the STS-1 and STS-2 entries have been interpolated to the altitudes of the Shuttle entry tracks and are shown in Fig. 6.

The winds during each flight were significant, but it is obvious from the figures that winds from flight 2 were much

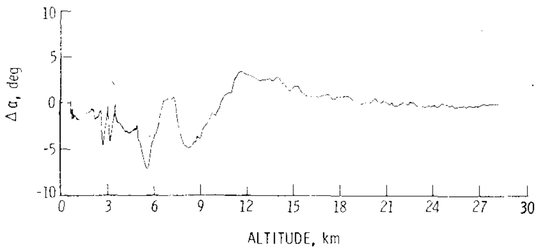

Fig. 7 STS-2 angle-of-attack difference due to wind.

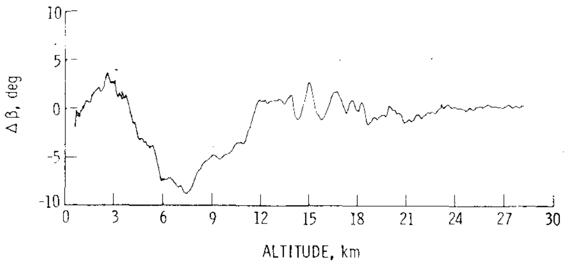

Fig. 8 STS-2 sideslip angle difference due to wind.

larger than those encountered on flight 1, particularly within the lower 15 km. Above 30 km, where the wind information provided by LAIRS is necessarily less accurate because of the distance of the Shuttle from the measuring stations, the vehicle velocity is high and thus the winds have little effect on the total velocity. The effect of the high winds from flight 2 on the trajectory parameters is partially illustrated by the results shown in Figs. 7 and 8. The two figures show the variation of errors in angle of attack and sideslip assuming the winds to be unknown and thus set to zero. Since such errors would be intolerable for the flight control of the Shuttle, the winds must be accurately determined. Other uses for accurate atmospheric information could be illustrated via their use in computing such parameters as Mach number, dynamic pressure, and aerodynamic coefficients. However, it is sufficient to say that the temperature, density, pressure, and wind parameters are combined with the best estimated trajectory parameters and other flight measurements to analyze Shuttle aerodynamic and performance characteristics during entry. These analyses will continue after each flight until the Shuttle flight envelope has been properly defined, so the requirement for atmospheric information exists for each flight.

Concluding Remarks

An accurate assessment of the ambient environment is an absolute necessity in order to properly evaluate the aerodynamics of the Shuttle. Until SUMS and SEADS provide a full-speed range air data system on future flights, the sounding data must be used for obtaining the required information.

Because of the importance of the air parameters, the sounding data have been independently reduced by NASA and NOAA using two different methods. It is somewhat comforting that these two sets of reduced data are in good agreement.

The results of this work are published, along with the vehicle state parameters and distributed to all of the agencies involved in assessing Orbiter entry performance.

Acknowledgments

The development and programming of the atmospheric analysis code described was accomplished under Contract NAS1-16412 with the Computer Sciences Corporation. Much of the work was done by members of their staff, including D.E. Boland Jr., T. Lee, J.O. Cappellari Jr., A. K. Kapoor, and R. A. Kuseski.

References

[1] Hinson, E., "SUMS Preliminary Design and Data Analysis Development," NASA CR 165696, May 1981.

[2] Siemers, P.M. III and Larson, T.J., "Space Shuttle Orbiter and Aerodynamic Testing," *Journal of Spacecraft and Rockets,* Vol. 16, No. 4, July-Aug. 1979, pp. 223-231.

[3] Boland, D.E. Jr. and Lee, T., "Langley Atmospheric Information Retrieval System (LAIRS) System—Description and User's Guide," NASA CR 3529, March 1982.

[4] Price, J.M. and Blanchard, R.C., "Determination of Atmospheric Properties for STS-1 Aerothermodynamic Investigations," AIAA Paper 81-2430, Nov. 1981.

[5] Compton, H.R., Findlay, J.T., Kelly, G.M., and Heck, M.L., "Shuttle STS-1 Entry Trajectory Reconstruction," AIAA Paper 81-2459, Nov. 1981.

[6] COSPAR Working Group, *COSPAR International Reference Atmosphere 1972,* (CIRA 1972) Akademie-Verlag, Berlin, 1972.

[7] Valley, S.L. (ed.), *Handbook of Geophysics and Space Environments*, Air Force Cambridge Research Laboratories, 1965.

[8] Jacchia, L.G., "Revised Static Models of the Thermosphere and Exosphere with Empirical Temperature Profiles," Smithsonian Astrophysical Observatory Special Rept. No. 332, 1971.

[9] Roberts, E.R. Jr., "An Analytical Model for Upper Atmosphere Densities Based Upon Jacchia's 1970 Models," *Celestial Mechanics*, Vol. 4, No. 3, Dec. 1971, pp. 368-377.

[10] Price, J.M., "Atmospheric Modeling for Shuttle Aerothermodynamic Investigations," *Proceedings of Workshop on Satellite Drag*, NOAA Environmental Research Laboratories, May 1982, pp. 22-30.

[11] Compton, H.R., Scallion, W.J., Suit, W.T., and Schiess, J.R., "Shuttle Entry Performance and Stability and Control Derivatives Extraction from Flight Measurement Data," AIAA Paper 82-1317, Aug. 1982.